Complete description of photon trajectories in the Kerr-Newman space-time

1981 J. Phys. A: Math. Gen. 14 1931

(http://iopscience.iop.org/0305-4470/14/8/018)

J. Phys. A: Math. Gen. **14** (1981) 1931–1942. Printed in Great Britain

Complete description of photon trajectories in the Kerr–Newman space–time

M Calvani† and R Turolla‡

† Institute of Astronomy, University of Padova, Italy
‡ International School for Advanced Studies, Trieste, Italy

Received 28 November 1980, in final form 9 February 1981

Abstract. We give the complete description of null trajectories in the Kerr–Newman space–time in terms of the parameters of the source and of the constants of motion. The conditions for orbital and vortical motion are studied in detail and we are able to give the locus of turning points for any choice of the parameters.

1. Introduction

Although there is yet no definite proof of the existence of black holes it is widely believed that the outcome of a gravitational collapse is described by the family of Kerr–Newman solutions, which are parametrised by the mass M, the specific angular momentum a and the charge Q of the source.

The geodesic properties of the Schwarzschild ($a = Q = 0$) and Kerr ($Q = 0$) solutions were investigated in great detail (see Sharp 1979 for references) in connection with their astrophysical relevance, while the more general Kerr–Newman space-time was left aside. In fact it appears that 'real' black holes do not have a net amount of charge, although this possibility has not yet been ruled out.

In this paper we complete and extend previous works (Carter 1968, Johnston and Ruffini 1974, Young 1976, Dadhich and Kale 1977a,b, de Felice *et al* 1980a,b, Calvani *et al* 1980) giving the complete description of null geodesics outside the equatorial plane as radiation propagates to a distant observer along these trajectories. For completeness we shall consider either black holes ($a^2 + Q^2 \leqslant M^2$) or naked singularities ($a^2 + Q^2 > M^2$) and we shall refer to the extended manifold ($-\infty < r < +\infty$).

In § 2 we shall study the locus of turning points as a function either of the parameters of the source or of the constants of motion of the null geodesics; in § 3 we shall recall the conditions for orbital and vortical motion which will be studied in §§ 4 and 5.

The physical results which are described in the last section are new as the behaviour of null geodesics outside the equatorial plane in the KN metric, as well as the existence of bound orbits, is studied in detail here for the first time.

2. The r motion

In the Kerr–Newman space-time the r motion of photons is described by the equation (Sharp 1979)

$$\Sigma^2 \dot{r}^2 = [(r^2 + a^2) - al]^2 - \Delta K \tag{1}$$

0305-4470/81/081931 + 12$01.50

where

$$\Sigma = r^2 + a^2 \cos^2 \vartheta \qquad \Delta = r^2 - 2Mr + a^2 + Q^2.$$

In the above formulae M, Q and a are the parameters which describe the background metric; M is the mass of the source, Q its charge and a its specific angular momentum. The parameters l and K are constants which describe the particle motion; l is the azimuthal angular momentum and K (Carter's fourth constant of motion, which is always non-negative) is related to the square of the total angular momentum at infinity (de Felice 1980). Note that the particle energy does not appear explicitly as it can be scaled to unity by an appropriate choice of the affine parameter.

In order to study the behaviour of null orbits we shall search for the locus of turning points, which are solutions of the equation $\dot{r} = 0$. From equation (1) one has

$$K = [(r^2 + a^2) - al]^2/\Delta \equiv K_t \tag{2}$$

which represents a three-parameter family of curves in the $(K - r)$ plane. The study of this function is rather long and involved and therefore here we shall give only an outline of the procedure. Many figures are inserted in order to visualise and to clarify the physical dependence on the parameters.

To know how the curves (2) change by varying the parameters we first study the functions

$$l = (r^2 + a^2)/a \equiv l_z \tag{3a}$$

$$l = [-r^3 + 3Mr^2 - r(a^2 + 2Q^2) - Ma^2]/a(r - M) \equiv l_e \tag{3b}$$

which give respectively the zeros and the extrema of K_t. Note that the zeros of K_t are also extrema. Equation (3a) is simply a parabola in the $(l - r)$ plane, so we are left with the function (3b) whose zeros and extrema are given respectively in the $(Q - r)$ plane by

$$Q^2 = (-r^3 + 3Mr^2 - Ma^2 - ra^2)/2r \equiv Q_1^2 \tag{4a}$$

and

$$Q^2 = [(r - M)^3 + M(M^2 - a^2)]/M \equiv Q_2^2. \tag{4b}$$

The zeros and extrema of Q_1^2 are respectively given, in the $(a - r)$ plane, by:

$$a^2 = r^2(3M - r)/(r + M) \equiv a_2^2 \tag{5a}$$

$$a^2 = r^2(2r - 3M)/M \equiv a_3^2. \tag{5b}$$

Q_2^2 has always a flex point at $r = M$ but no extrema and its zeros are along

$$a^2 = r(r^2 - 3Mr + 3M^2)/M \equiv a_4^2. \tag{6}$$

The functions a_2^2, a_3^2 and a_4^2 are shown in figure 1†.

We have now some kind of 'Chinese boxes': for any value of the parameter a figure 1 allows us to draw the functions Q_1^2 and Q_2^2; this is done in figure 2. For any value of Q we can now, with the help of figure 2, draw the function l_e which gives the extrema of K_t; this is done in figure 3 where also l_z, which gives zeros and extrema of K_t, is shown. Note that either l_e or l_z crosses the l axis at $l = a$. Moreover, it is easy to show that in the black hole case (figure 3(c)) the radius r_- of the inner horizon is always smaller than the radius

† In all the figures we assume the mass M of the source as unit of length for the r coordinate, therefore M does not appear explicitly as a parameter.

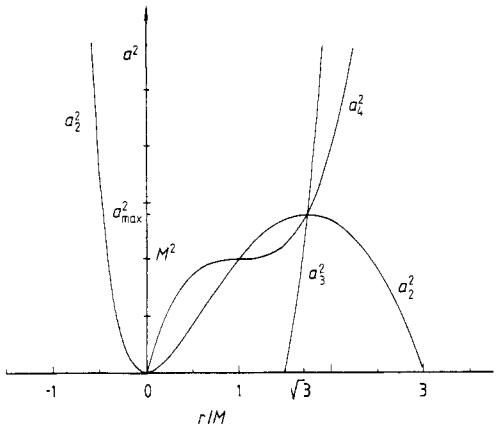

Figure 1. The functions a_2^2, a_3^2 and a_4^2 are shown. They intersect at $r = M\sqrt{3}$ where $a^2 = 3\sqrt{3}(2-\sqrt{3})M^2 \equiv a_{max}^2$.

where l_e is maximum i.e. that

$$r_- = M - (M^2 - a^2 - Q^2)^{1/2} < r_{max} = M - [M(M^2 - Q^2 - a^2)]^{1/3}.$$

We still need to know where the divergences of K_t lie; this occurs where $\Delta = 0$, which is also the condition which gives the horizons in the black hole case. It implies

$$Q^2 = 2Mr - r^2 - a^2 \equiv Q_d^2 \tag{7}$$

whose zeros are along

$$a^2 = 2Mr - r^2 \equiv a_1^2. \tag{8}$$

In figure 4 are shown the functions (7) and (8) and the function

$$Q^2 = r^2 - 2Mr \equiv Q_e^2$$

which gives the intersections of the ergosphere with the equatorial plane.

We have now all that is needed (figures 1–4) to draw the function K_t for any choice of the parameters, and therefore we are now able to investigate the locus of turning points for photons. This will be done in the last section as we believe it is useful to recall first the conditions for orbital and vortical motion to occur and to analyse them.

3. Conditions for orbital and vortical motion

In this section we shall briefly recall the results obtained in the Kerr metric (de Felice and Calvani 1972, Bičák and Stuchlík 1976) concerning the description of the ϑ motion. Those results still hold in the Kerr–Newman metric as the charge Q does not affect the ϑ equation of motion which reads:

$$\Sigma^2 \dot{\vartheta}^2 = K - \frac{1}{\sin^2 \vartheta}(a \sin^2 \vartheta - l)^2. \tag{9}$$

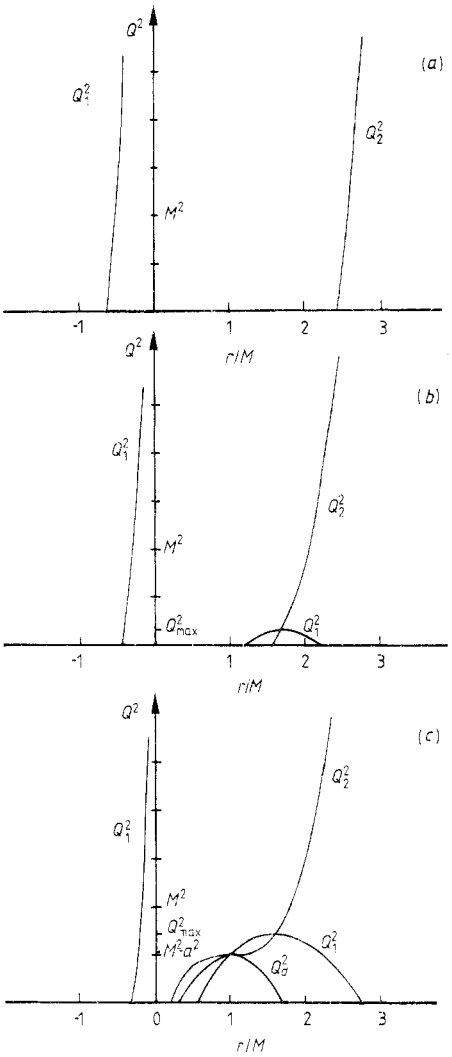

Figure 2. The functions Q_1^2, Q_2^2 and Q_a^2 are shown for the three ranges of interest of a^2 (see figure 1). (*a*) $a^2 > a^2_{max}$. The figure is drawn for $a^2 = 2M^2$. (*b*) $M^2 < a^2 < a^2_{max}$ ($a^2 = 1.2M^2$). (*c*) $a^2 < M^2$ ($a^2 < 0.5M^2$). Cases (*a*) and (*b*) refer to naked singularities while (*c*) refers to black holes (see figure 4). Note that l_e has zeros at $r > 0$ only if $Q^2 < Q^2_{max}$ and that $Q^2_{max} > 0$ only if $a^2 < a^2_{max}$.

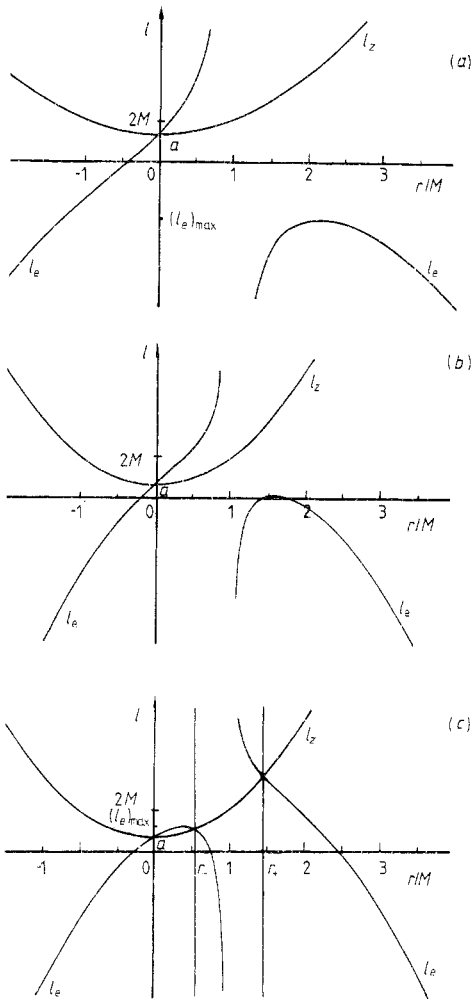

Figure 3. The functions l_e and l_z are shown. They both intersect $r = 0$ at $l = a$. (*a*) $a^2 > a^2_{max}$ and $Q^2 > Q^2_{max}$ ($a^2 = 2M^2$, $Q^2 = 0.5M^2$), (*b*) $a^2 < M^2 < a^2_{max}$ and $(M^2 - a^2) < Q^2 < Q^2_{max}$ ($a^2 = 0.5M^2$, $Q^2 = 0.7M^2$), (*c*) $a^2 < M^2$ and $Q^2 < (M^2 - a^2)$ ($a^2 = 0.5M^2$, $Q^2 = 0.3M^2$). The two vertical lines denote the horizons $r_\pm$. Cases (*a*) and (*b*) refer to naked singularities while (*c*) refers to black holes.

One can prove that there are two types of trajectories: those that cross the equatorial plane (orbital motion) and those that never cross it and are confined between two hyperboloids ϑ = constant (vortical motion). The last ones are the only orbits entitled to enter the r-negative part of the manifold through the ring singularity in the equatorial plane.

The conditions for orbital and vortical motion can be given in terms of the constants of motion K and l and of the parameter a. For vortical motion the following set of

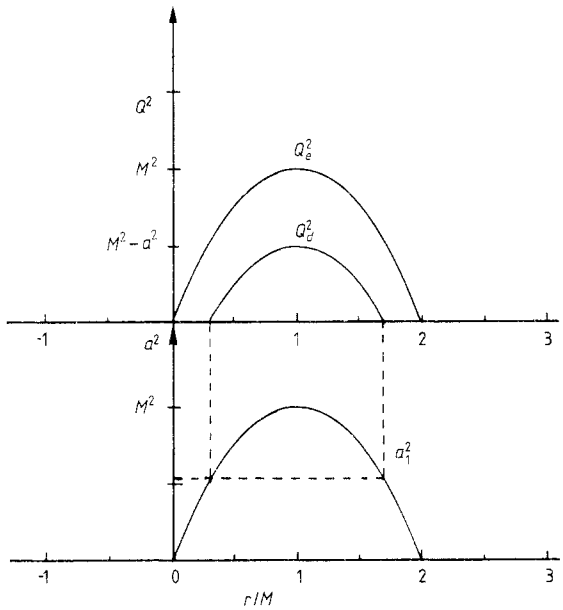

Figure 4. The functions a_1^2, Q_d^2 and Q_e^2 are shown. Black holes exist only in the range $a^2 \leqslant M^2$ and $Q^2 \leqslant (M^2 - a^2)$.

conditions must hold:

$$K \leqslant (l-a)^2 \tag{10a}$$

$$K \geqslant -4al \tag{10b}$$

$$-a < l < a. \tag{10c}$$

These constraints are simultaneously satisfied in the dotted region of figure 5. In the region where

$$K \geqslant (l-a)^2 \tag{10d}$$

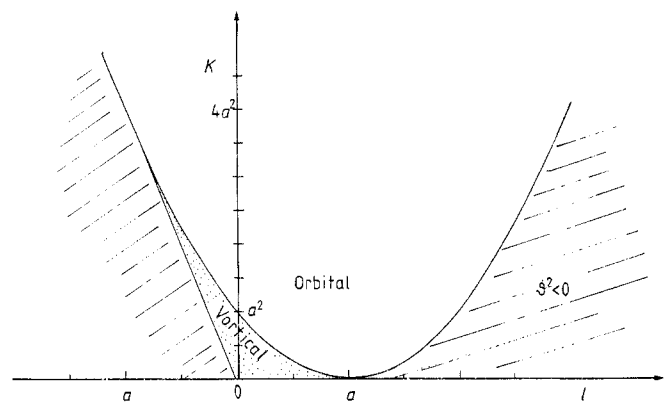

Figure 5. The constraints for orbital and vortical motion are shown. In the shaded area motion is forbidden as there $\dot{\vartheta}^2 < 0$. Vortical motion occurs only in the dotted area.

the motion is of the orbital type. The shaded area in figure 5 is forbidden as there $\dot{\vartheta}^2 < 0$, or the two $(\sin^2\theta)$ – roots of $\dot{\theta}^2 = 0$ are both greater than 1.

The particular value $K = (l-a)^2$ corresponds to motion in the equatorial plane and this case has been analysed by Calvani *et al* (1980). Conditions (10) will be studied in detail in the following sections.

4. Orbital motion

Condition (10*d*) for orbital motion together with equation (2) can be written as

$$(a^2-\Delta)Z^2 - 2r^2aZ + r^4 \geqslant 0 \tag{11}$$

where $Z = (l-a)$. This is satisfied, according to the sign of $(a^2-\Delta)$, when $Z_- < Z < Z_+$ or $Z > Z_+$ and $Z < Z_-$; $Z_\pm$ are the roots of equation (11)

$$Z_\pm = r^2/(a \pm \sqrt{\Delta}). \tag{12}$$

$Z_\pm$ vanish only at $r = 0$ while their extrema are at $r = 0$ and along the curves

$$Q^2 = \tfrac{1}{2}[-r^2 + 3Mr - a^2 - a\sqrt{a^2 + 2r(r-m)}] \equiv \bar{Q}^2 \tag{13a}$$

and

$$Q^2 = \tfrac{1}{2}[-r^2 + 3Mr - a^2 + a\sqrt{a^2 + 2r(r-M)}] \equiv \tilde{Q}^2. \tag{13b}$$

It can be proved that $\tilde{Q}^2$ gives the extrema of Z_- while $\bar{Q}^2$ gives those of Z_+ for $r < 0$, $r > M$ and those of Z_- for $0 < r < M$; moreover, $r = 0$ is a maximum for Z_- and a minimum for Z_+.

Let us now study $\bar{Q}^2$ and $\tilde{Q}^2$; the following properties hold:

$$\tilde{Q}^2 = 0 \quad \text{and} \quad \bar{Q}^2 = -a^2 \quad \text{at } r = 0$$

$$\tilde{Q}^2 = M^2 \quad \text{and} \quad \bar{Q}^2 = (M^2 - a^2) \quad \text{at } r = M.$$

The zeros of $\tilde{Q}^2$ and $\bar{Q}^2$ are at $r = 0$ and along the curve

$$a^2 = r(r-3M)^2/4M \equiv a_8^2; \tag{14}$$

it is easy to show that a_8^2 gives the zeros of $\tilde{Q}^2$ for $r > 3M$ and those of $\bar{Q}^2$ for $0 < r < 3M$, while $r = 0$ is a zero only for $\tilde{Q}^2$. It can be proved also that

$$a^2 = r(2r-3M)^2/4M \equiv a_9^2 \tag{15}$$

gives the extrema of $\tilde{Q}^2$ for $0 < r < M/2$, $r > 3M/2$ and those of $\bar{Q}^2$ for $M/2 < r < 3M/2$, together with $r = M$. One finds that $r = M$ is a maximum for $\bar{Q}^2$ when $M^2 < 4a^2$ and a minimum when $M^2 > 4a^2$.

The functions a_8^2, a_9^2 and

$$a^2 = -2r(r-M) \equiv a_{10}^2 \tag{16}$$

(the locus where $\bar{Q}^2 = \tilde{Q}^2$) are plotted in figure 6. Figures 7 and 8 show respectively the behaviour of $\tilde{Q}^2$, $\bar{Q}^2$ and of $(l_0)_\pm = Z_\pm + a$. The relevance of $(l_0)_\pm$ as far as the description of null trajectories is concerned will be discussed in the last section.

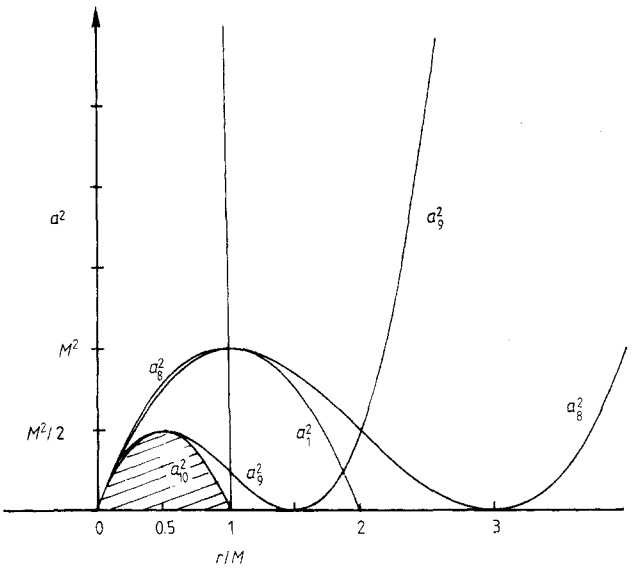

Figure 6. The functions a_1^2, a_8^2, a_9^2 and a_{10}^2 are shown. The functions $\bar{Q}^2$ and $\tilde{Q}^2$ are real outside the shaded area enclosed by a_{10}^2.

5. Vortical motion

Condition (10*b*) and equation (2) can be combined to give

$$(r^2+a^2-al)^2/\Delta \geqslant -4al \tag{17}$$

or equivalently

$$a^2l^2+2al[2\Delta-(r^2+a^2)]+(r^2+a^2)^2 \geqslant 0 \tag{18}$$

which is satisfied outside the horizons (when they exist) only for $l<0$. The roots of equation (18) are

$$(l_v)_\pm = \{-(\Delta+Q^2-2Mr) \pm 2[\Delta(Q^2-2Mr)]^{1/2}\}/a. \tag{19}$$

A detailed study of the functions $(l_v)_\pm$ is quite long and therefore we briefly describe here their main properties:

(i) the functions $(l_v)_\pm$ have no zeros and are always negative when $\Delta>0$, as can be seen from the coefficients of equation (18);

(ii) at $r=Q^2/2M$ the functions $(l_v)_+$ and $(l_v)_-$ have the same value i.e.

$$(l_v)_+ = (l_v)_- = -(a^2+Q^4/4M^2)/a < -a;$$

(iii) from equation (17) it is easy to see that at $l=-a$ the curves $(l_0)_-$ and $(l_v)_+$ are tangent, as shown in figure 8;

(iv) the maximum of $(l_v)_+$, denoted by $(l_v)_{\max}$ in figure 8, lies on l_e, as can be seen by studying the derivative of $(l_v)_+$;

(v) at $r=0$ the functions (19) take the following values

$$l_1 = (l_v)_+ = \{-(a^2+2Q^2)+2[Q^2(a^2+Q^2)]^{1/2}\}/a > -a$$

$$l_2 = (l_v)_- = \{-(a^2+2Q^2)-2[Q^2(a^2+Q^2)]^{1/2}\}/a < -a.$$

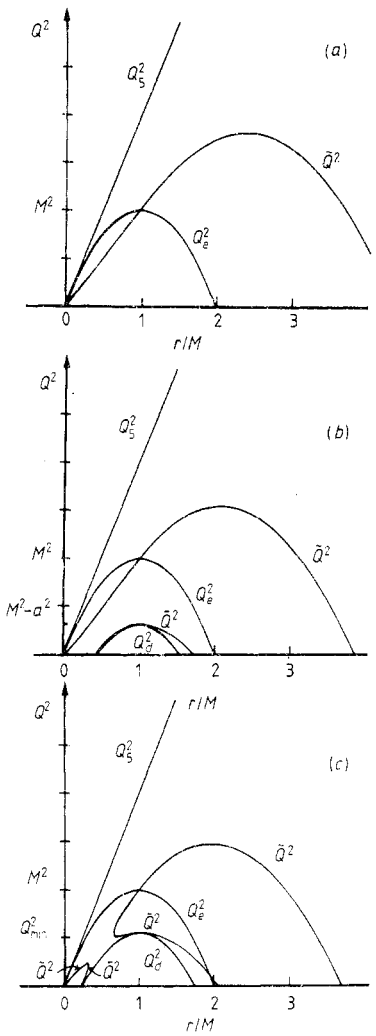

Figure 7. The functions Q_e^2, Q_d^2, $\tilde{Q}^2$, $\tilde{Q}^2$ and $Q^2=2Mr\equiv Q_5^2$ are shown. (*a*) $a^2>M^2$ ($a^2=2M^2$), (*b*) $M^2/2<a^2<M^2$ ($a^2=0.75M^2$), (*c*) $a^2<M^2/2$ ($a^2=0.45M^2$).

For any choice of l such that $l_1<l<l_2$

$$(K_t)_{r=0}\equiv K_0=a^2(l-a)^2/(a^2+Q^2)<-4al$$

and therefore in this range of l only vortical motion is allowed (see figure 5). Moreover $(l-a)^2>K_0$, and this result is useful in drawing figures 9 and 10 and to discriminate between orbital and vortical motion.

6. Discussion

The considerations developed in the previous sections allow us to draw the functions l_e, l_z, $(l_0)_\pm$ and $(l_v)_\pm$ for any choice of the parameters. All these functions are plotted

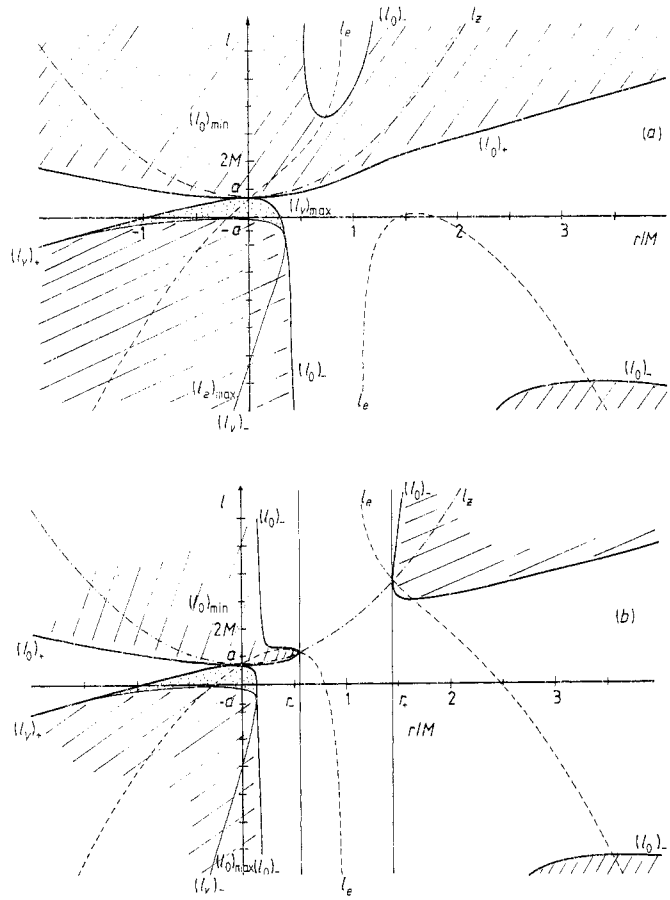

Figure 8. The functions l_e, l_z, $(l_0)_\pm$ and $(l_v)_\pm$ are drawn together. They allow us to draw the locus of turning points K_r and to distinguish between orbital and vortical motion. (*a*) $a^2 < M^2$ and $Q^2 > (M^2 - a^2)$ ($a^2 = 0.5M^2$, $Q^2 = 0.7M^2$), (*b*) $a^2 < M^2$ and $Q^2 < (M^2 - a^2)$ ($a^2 = 0.5M^2$, $Q^2 = 0.3M^2$). The full heavy curve marks $(l_0)_\pm$; the full light curve marks $(l_v)_\pm$; the chain curve marks l_z and the broken curve marks l_e. Note that all the curves intersect at $r = r_\pm$.

together in figure 8 in order to obtain first some physical information on the ϑ motion of photons and then to draw and study the locus of radial turning points (equation (2)). Note that all the curves cross on $\Delta = 0$.

From conditions (10) and figure 5 it is easy to verify that in the shaded part of figure 8 it is either $\dot{\vartheta}^2 < 0$ or $\sin^2 \vartheta > 1$ so that there no motion is allowed, and that the conditions for vortical motion are fulfilled only in the dotted area. The following properties on the motion may now be deduced.

(i) For $0 < l < a$ there are two ϑ turning points unless $K = 0$; in this case the motion is on an hyperboloid $\vartheta = \text{constant}$ with $\sin^2 \vartheta = l/a$.

(ii) For $(l_v)_{\max} < l < 0$ there are two turning points where $(l_v)_{\max} = \max(l_v)_+$.

(iii) Only those photons with $(l_v)_{\max} < l < a$ are entitled to cross the ring singularity and go to infinite negative r: whether this occurs depends on the value of K as will be shown later.

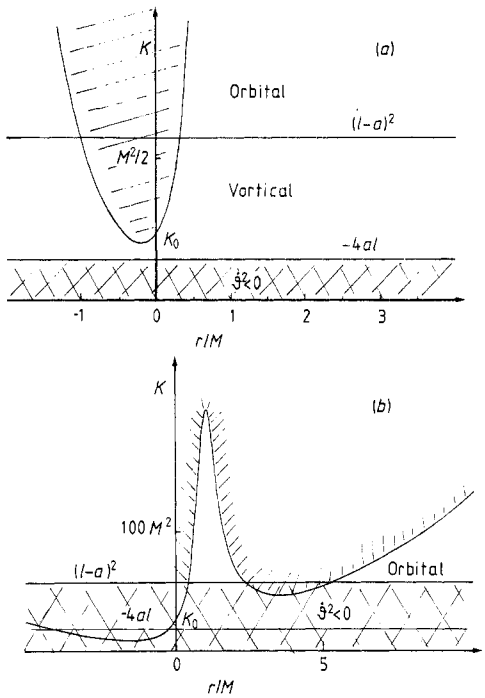

Figure 9. The locus of turning points in the naked singularity case. (*a*) $a^2<M^2$, $Q^2>(M^2-a^2)$, $a>l>(l_v)_{\max}$ ($a^2=0.5M^2$, $Q^2=0.7M^2$, $l=-0.05M$). The line $K=(l-a)^2$ separates the regions where orbital and vortical motion occur. In this case vortical trajectories can reach the r-negative part of the manifold as no turning points are met. (*b*) $l<(l_0)_{\max}$ ($l=-7M$). In this case only orbital motion is allowed. Note that bound orbits can exist around the singularity. The shaded part of the figure is forbidden to motion as there either $\dot{\vartheta}^2$ or $\dot{r}^2$ is negative.

(iv) K_t has zeros only for $l>a$ and therefore, for $l>a$, radial barriers prevent photons from reaching the $r=0$ disc (whose boundary is the ring singularity).

(v) For $l<(l_v)_{\max}$ there are values of K for which $\dot{\vartheta}^2<0$ (see figure 9) and photons cannot reach the $r=0$ disc.

More information about the radial motion can be read off from the graphs of the locus of radial turning points. In figures 9 and 10 we have drawn the function K_t for several values of the parameters and in the most interesting cases, making use of the curves in figure 8. In the shaded parts of figures 9–10, $\dot{r}^2<0$; the region where $\dot{\vartheta}^2<0$ is also shown (see also figure 5).

The following points are of interest.

(i) In the black hole case photons coming from infinity are not able to cross the outer horizon when $l>(l_e)_{\max}$ as they always find a turning point before; when $l<(l_e)_{\max}$ photons can cross the horizons depending on the value of K.

(ii) In the naked singularity case only some photons moving with vortical motion go through the ring singularity, depending on the values of the parameters as has been pointed out before.

(iii) The existence of bound orbits is very interesting (in particular of orbits with $r=$ constant) in the naked singularity case; this happens for example when $(l_0)_{\min}<l<$

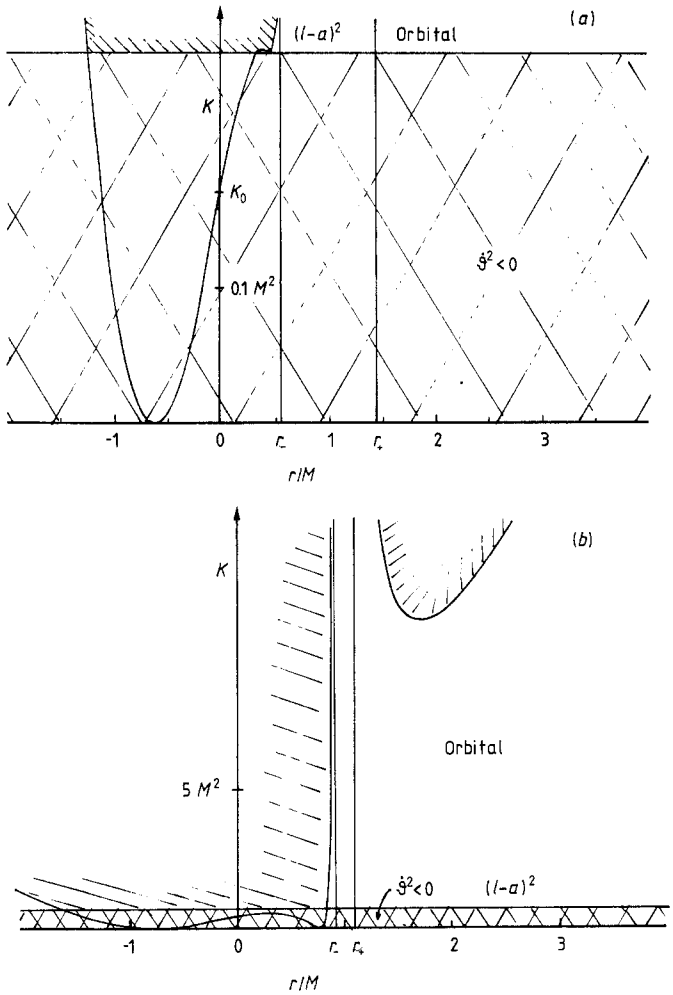

Figure 10. The locus of turning points in the black hole case. (*a*) $l > (l_e)_{\max}$ ($a^2 = 0.5M^2$, $Q^2 = 0.49M^2$, $l = 1.5M$). Repulsive barriers prevent photons from reaching $r = 0$. (*b*) $a^2 = 0.4M^2$, $Q^2 = 0.2M^2$ and $l = 1.23M$. For this value of l bound orbits exist beyond the inner horizon.

$(l_e)_{\max}$. The existence of such orbits has already been pointed out by Calvani *et al* (1980), de Felice and Calvani (1979) and de Felice (1979). These orbits exist also in the black hole case under the inner horizon if the following conditions hold: $M^2 < 4a^2$ (so that $r = M$ is a maximum for Q^2, see figure 7), $Q^2_{\min} < Q^2 < (M^2 - a^2)$ (so that $(l_0)_-$ has a maximum and a minimum before r_-) and l must be between this maximum of $(l_0)_-$ and $(l_e)_{\max}$ (see figure 10(*b*)); one can show that these orbits do not exist outside the outer horizon.

Owing to the presence of several parameters (a, Q, l, K) the description of all possible cases of motion turns out to be quite complicated; anyhow the procedure we have used and the figures shown in this paper make it possible to draw the locus of radial turning points for any value of the parameters and therefore allow one to have a deep insight into the behaviour of photon trajectories in the Kerr–Newman space–time.

Acknowledgments

We should like to thank Dr N Sharp for having brought to our attention this particular problem. We should also like to thank Dr Patrizia Di Cola for her help in drawing the figures. This work was supported by the Italian National Council of Research (CNR).

Note added in proof. Thanks are due to Dr Stuchlik for useful comments.

References

Bičák J and Stuchlík Z 1976 *Bull. Astron. Inst. Czeck.* **27** 129
Calvani M, de Felice F and Nobili L 1980 *J. Phys. A: Math. Gen.* **13** 3213
Carter B 1968 *Phys. Rev.* **174** 1559
Dadhich N and Kale P P 1977a *J. Math. Phys.* **18** 1727
—— 1977b *Pramaña* **9** 71
de Felice F 1979 *Phys. Rev.* D **19** 451
—— 1980 *J. Phys. A: Math. Gen.* **13** 1701
de Felice F and Calvani M 1972 *Nuovo Cimento* B **10** 447
—— 1979 *Gen. Rel. Grav.* **10** 335
de Felice F, Nobili L and Calvani M 1980a *J. Phys. A: Math. Gen.* **13** 2401
—— 1980b *J. Phys. A: Math. Gen.* **13** 3635
Johnston M and Ruffini R 1974 *Phys. Rev.* D **10** 2324
Sharp N 1979 *Gen. Rel. Grav.* **10** 659
Young P J 1976 *Phys. Rev.* D **14** 3281